

The isotropy problem of Ultra-high energy cosmic rays: the effects of anisotropic transport

RAHUL KUMAR, DAVID EICHLER

Physics Department, Ben-Gurion University, Be'er-Sheva 84105, Israel

rahulitk@gmail.com

Abstract: We show that particle drift may play an important role in the transport of ultra-high energy cosmic rays (UHECRs) and their measured anisotropy, particularly when the transport is anisotropic. Drift and anisotropic diffusion has not been adequately included in previous studies. To fully account for the discreteness of UHECR sources in space and time, the Monte Carlo method is used to randomly place sources in the Galaxy and calculate the anisotropy of UHECR flux, given specific realisations of source distribution. We show that reduction in the rate of cross-field transport reduces the anisotropy. However, if the cross-field transport is very small, drift of UHECRs in the Galactic magnetic field (GMF) becomes the dominant contributor to the anisotropy. Test particle simulations further illustrate the effect of drift and verify our analytical calculation. The surprisingly low anisotropy measured by Auger can be interpreted as intermittency of UHECR sources, without invoking a flat source distribution and/or a high source rate.

Keywords: UHECRs, anisotropy, CRs

1 Introduction

It is widely suspected that the abrupt flattening of the cosmic ray (CR) spectrum above 4 EeV, the so-called ankle [16] of the CR spectrum, is due to transition from the Galactic to extragalactic sources. The sources of EeV UHECRs is still an open question. Blast waves from supernova remnants are believed to be unable to accelerate CR protons to energy beyond $10^{14.5}$ eV [14], though [13] has argued that higher energies may be attainable on equatorial drift trajectories if the magnetic field is sufficiently ordered. As proposed by [15], GRBs occurring in our Galaxy are possible sources for CRs up to the ankle. Once injected by the sources, propagation of CRs from source to the Earth would depend only on the interaction of CRs with the interstellar medium regardless of the nature of the sources.

Recently the [17] published their measurement of large scale anisotropy in the arrival direction of UHECRs. In a previous paper [19] (henceforth referred to as PE11) showed that the anisotropy predicted by an isotropic diffusion model due to discrete sources in the Galaxy is on average much higher than the measured value. The premises of their model led the authors to conclude that a) the mean free path of the UHECRs is small compared to the proton Larmor radius, or b) intermittency is an important factor and we are living in a rare lull in UHECR production, or c) majority of sub ankle CRs have extragalactic origin. Estimates of anisotropy in several other models [7, 11, e.g.] are also higher than the observed limit for light sub-ankle primaries. We refer to this discrepancy between measured value and theoretical models as the UHECR isotropy problem.

In this paper we consider gyration of CR protons in the GMF which makes their transport anisotropic. We show that reduced cross-field transport significantly reduces the anisotropy of UHECRs compared to the isotropic diffusion model discussed in PE11, and appears to strengthen the case for intermittency as an answer to the isotropy problem. Specifically, the expected anisotropy is higher than

observed even for anisotropic diffusion, but the probability is increased that downward fluctuations, either due to lulls in production or due to nearby sources that offset the expected global Galactic anisotropy, will bring the instantaneous anisotropy into accord with observations. We further show that when drift of UHECRs in the GMF is taken into consideration, total anisotropy increases significantly, partially cancelling the reduction due to anisotropic transport. We present results from test particles simulation of UHECRs in the continuum source limit to illustrate the effect of drift.

2 propagation of UHECRs from galactic sources: anisotropic diffusion

The turbulent GMF causes UHECRs to scatter and the propagation of charged CRs in the turbulent GMF is governed by the diffusion equation. The turbulence in the GMF is assumed to be isotropic. The regular component of the GMF (directed along the spiral arms), however, breaks the isotropy of diffusion and cross field transport of CRs is reduced [10] due to the gyration of UHECR protons.

We assume the classical scattering limit for the diffusion of charged particles in a magnetic field, that is to say CRs spiral in the regular GMF between instantaneous isotropic scattering events. In this limit, diffusion coefficients parallel and perpendicular to the magnetic field at any given energy are $D_{\parallel} = c\lambda_{mfp}/3$ and $D_{\perp} = c\lambda_{mfp}/[3(1 + \lambda_{mfp}^2/r_L^2)]$ respectively [4], where r_L is Larmor radius, c is the speed of light, and λ_{mfp} is the mean distance travelled by UHECRs between two subsequent random scattering events. This implies that $D_{\parallel} \propto 1/D_{\perp}$ (it could be that D_{\parallel} and D_{\perp} are weakly correlated due to the complicated magnetic field lines in the Galaxy, so we keep our discussion more general and treat D_{\parallel} and D_{\perp} as two independent parameters).

At 10^{18} eV the composition of UHECRs is light, though not necessarily dominated by protons [3, 1]. We assume

in this paper that UHECRs in the 1-4 EeV energy band is mostly protons. A heavier composition of average nuclear charge Z at energy E_Z would behave like a proton dominated UHECRs of energy $E = E_Z/Z$, and as shown later, would imply a lower anisotropy than a proton dominated UHECRs at the same energy. As in PE11, we use Larmor radius of protons in $10 \mu G$ as a scale in this paper.

2.1 Anisotropic Diffusion in Disk Geometry

We assume that the GMF is axisymmetric and we work in galacto-centric polar coordinate ρ, ϕ , and z . We assume that UHECRs are instantly released at $t = t_0$ from point-like sources such as GRBs. The differential density of UHECRs released from a source located at $(\rho = \rho_0, \phi = 0)$ obeys the diffusion equation which can be written in galactocentric cylindrical polar coordinate as,

$$\frac{\partial N}{\partial t} + \frac{N}{T} = \frac{\partial}{\partial \rho} \rho D_{\perp} \frac{\partial N}{\partial \rho} + \frac{\partial}{\partial \phi} D_{\parallel} \frac{\partial N}{\partial \phi} + \frac{\partial}{\partial z} D_{\perp} \frac{\partial N}{\partial z} + Q(E) \delta(t) \delta(\rho - \rho_0) \delta(\phi) \delta(z) / \rho, \quad (1)$$

where $D_{\rho\rho} = D_{zz} = D_{\perp}$, $D_{\theta\theta} = D_{\parallel}$, T is the loss time for photo-secondary production, and $Q(E)$ is the differential production rate of UHECRs. Here the GMF is assumed to be toroidal.

UHECRs reaching a few Kpc out into the halo efficiently escape from the Galaxy because of weaker local GMF (moderating exponentially with distance from the Galactic plane). Escape from the Galaxy can be modelled by introducing absorbing boundary conditions $N(z \pm H) = 0$. For UHECRs, escape is the dominant loss process in the Galaxy, and in the steady state we expect their density to decrease linearly with z , from $N_0(\rho, \phi)$ in the Galactic plane to zero at $z = \pm H$. The diffusive escape in z -direction can thus be described using a loss time $\tau_{esc} = H^2/2D_{\perp}$. Since τ_{esc} , typically a few Myr, is much shorter than the energy loss time, T , which is $\gtrsim 10^8$, energy losses in UHECRs propagation can be ignored [5, 12]. Replacing the derivative of diffusive flux in the z -direction in equation 1 by catastrophic loss term with loss time τ_{esc} , we can write two dimensional diffusion equation for mid-plane density N_0 in ρ and ϕ (see PE11 for details). We find a series solution to the two dimensional diffusion equation for mid-plane density N_0 , which can be written as

$$N_0(\rho, \phi, t) = \frac{\Theta(t)}{2\pi D_{\perp} t} \frac{Q(E)}{H} \exp\left(-\frac{t}{\tau_{esc}} - \frac{\rho^2 + \rho_0^2}{4D_{\perp} t}\right) \times \left[\frac{1}{2} I_0(\tilde{\rho}) + \sum_{n=1}^{\infty} \cos(n\phi) I_{\nu(n)}(\tilde{\rho}) \right], \quad (2)$$

where $\tilde{\rho} = \rho\rho_0/2D_{\perp} t$, and $\nu(n) = n\sqrt{D_{\parallel}/D_{\perp}}$.

2.2 Anisotropy

The anisotropy in the UHECR intensity arises from the diffusive flux and is given by

$$\delta = \frac{I_{max} - I_{min}}{I_{max} + I_{min}} \simeq \left| \lambda_{\perp} \frac{\partial N_{tot}}{\partial \rho} \hat{\rho} + \lambda_{\parallel} \frac{\partial N_{tot}}{\rho \partial \phi} \hat{\phi} \right| / \left(N_{tot} + \frac{\lambda_{\perp}^2}{2\rho} \frac{\partial}{\partial \rho} \rho \frac{\partial N_{tot}}{\partial \rho} + \frac{\lambda_{\parallel}^2}{2\rho^2} \frac{\partial^2 N_{tot}}{\partial \phi^2} \right) \quad (3)$$

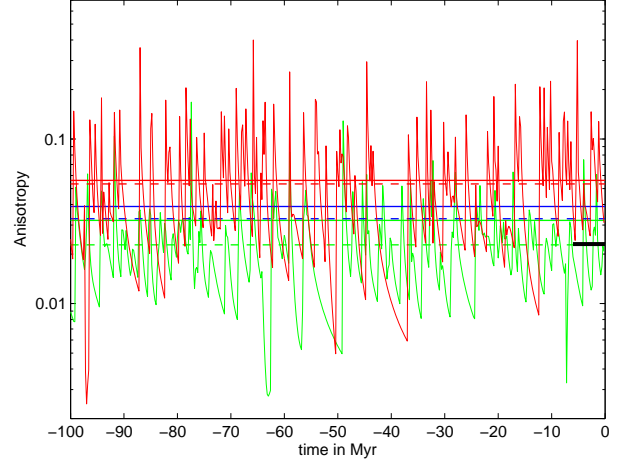


Figure 1: Temporal variation of the anisotropy and the mean anisotropy are shown for three different choices of diffusion parameters. case 1 (red): $D_{\perp} = D_{\parallel} = cr_L/3$ (isotropic diffusion); case 2 (blue): $2D_{\perp} = D_{\parallel} = cr_L/3$; case 3 (green): $10D_{\perp} = D_{\parallel}/3 = cr_L/3$. Here, and henceforth, energy is 2.4 EeV. Dashed lines of corresponding colors indicates the mean anisotropies and the solid lines are the mean anisotropies after adding the contribution from diamagnetic drift (the green dashed line coincides with the blue solid line). Here, and henceforth, the black bar on the right of the figure indicates the measured 99% upper limit by the Auger collaboration.

where $\lambda_{\parallel} = 3D_{\parallel}/c$, $\lambda_{\perp} = 3D_{\perp}/c$, and N_{tot} is the total density of UHECRs after summing the contributions of all sources that occurred in recent past.

To fully account for the discreteness of UHECRs sources in space and time, we use the Monte Carlo method to randomly place sources in the Galaxy with the given spatial probability distribution in galactocentric radius,

$$P(\rho_{GC}) = \frac{2\rho_{GC}}{\rho_0^2} \exp\left(-\frac{\rho_{GC}^2}{\rho_0^2}\right) \quad (4)$$

with scale $\rho_0 = 5$ kpc. This distribution is an approximation to the distribution of baryons and star formation in the Galaxy, which are reasonable proxies for the distribution of sources in the Galaxy.

Assuming by way of example that a GRB occurs in the Galaxy in every 1 Myr with the spatial distribution $P(\rho_{GC})$, we have plotted in figure 1 the temporal variation in the radial (i.e. galacto-radial) anisotropy for UHECR for three different choices of diffusion parameters; case 1: $D_{\perp} = D_{\parallel} = cr_L/3$, case 2: $2D_{\perp} = D_{\parallel} = cr_L/3$, and case 3: $10D_{\perp} = D_{\parallel}/3 = cr_L/3$. Case 1 is isotropic diffusion with $\lambda_{mfp} = r_L$, while in case 2 and 3 mean free path is r_L and $3r_L$ respectively with D_{\parallel} and D_{\perp} consistent with the classical scattering limit. Here, and henceforth, the halo size is $H = 5$ kpc and anisotropies are shown for UHECRs of energy 2.4 EeV. As evident from figure 1, the mean of anisotropy decreases with the decrease in D_{\perp} .

2.3 Drift in the Galactic Magnetic Field

UHECRs, as a gas of protons of number density N , collectively drift in an inhomogeneous magnetic field \mathbf{B} . The drift velocity, up to the first order in anisotropy, can be approximated by $E(\nabla N \times \mathbf{B})/3qNB^2$, which is also known as diamagnetic drift [6]. For UHECRs of energy several EeV, drift can have non-negligible contribution to the anisotropy. Since the GMF is assumed to be toroidal, drift would produce anisotropy in the direction perpendicular to the Galactic plane, proportional to the radial anisotropy. The mean of total anisotropy after adding UHECRs drift at Earth's location is shown in figure 1 as dashed lines. Drift is not significant for isotropic diffusion, but as the rate of transport in the radial direction decreases ($D_{\perp} \ll cr_L/3$) drift becomes the dominant contributor to the total anisotropy as compared to the radial anisotropy, implying that the reduction in the cross-field transport can not reduce the anisotropy indefinitely.

2.4 Test Particle Simulation

As discussed in the previous section, an inhomogeneous GMF would significantly alter the transport of UHECRs. Here we study the transport of UHECRs in the Galaxy by moving particles in computed trajectories in the GMF between two random scattering events to illustrate the effect of drift on anisotropy. We assume the toroidal GMF

$$\begin{aligned} B_{\phi}(\rho, z) &= B_0 B_{\phi}^{\rho}(\rho) B_{\phi}^z(z) \\ &= B_0 \exp(-(\max(\rho, \rho_c) - \rho_{\odot})/\rho_0 - |z|/z_0) \end{aligned}$$

where ρ_{\odot} is the radial location of the Sun ≈ 8.5 kpc, $B_0 = 10 \mu G$, and the parameters ρ_c , ρ_0 and z_0 were taken to be 3 kpc, 6 kpc and 1.5 kpc respectively [20].¹

Computing the anisotropy down to few percent at Earth would require large number of particles in the Earth's vicinity, and even larger to begin with from randomly placed sources. So we instead compute the anisotropy in the infinite source rate limit by computing time average velocity of all particles within distance r_L from solar circle, originating from a GRB at a distance d_s from the Galactic center. This is equivalent to the anisotropy at Earth due a homogeneous ring-like source of radius d_s . In figure 2, the anisotropy due to the ring-like sources is plotted against the radius of the ring. After taking the radial probability distribution $P(r_{GC})$ of ring-like sources into account, the net radial anisotropy for $\lambda_{mfp} = r_L(B_0)$ and $\lambda_{mfp} = 3r_L(B_0)$ is 2.8% and 2.1% respectively. Anisotropy in the direction perpendicular to the Galactic plane, which is due to drift in the toroidal GMF, is $\simeq 0.1\%$ for $\lambda_{mfp} = r_L(B_0)$, close to the drift calculated using first order diamagnetic drift approximation (fig. 1) in the case of discrete sources. If $\lambda_{mfp} = 3r_L(B_0)$, radial anisotropy goes down, however, drift becomes the dominant contributor to the total anisotropy, raising the total anisotropy to 5% (fig. 2). Drift becomes increasingly the dominant contributor to the total anisotropy as the transport of UHECRs becomes anisotropic, which also implies that drift become the dominant loss process for UHECRs.

We also consider the possibility that the GMF weakens rather slowly with distance from the galactic plane. It is commonly believed that the effect would be to decrease anisotropy, due to longer confinement of CRs in the Galaxy. However, as evident from table 1, the anisotropy increases as the halo magnetic field becomes stronger, because it then becomes harder for the scattering to suppress the drift.

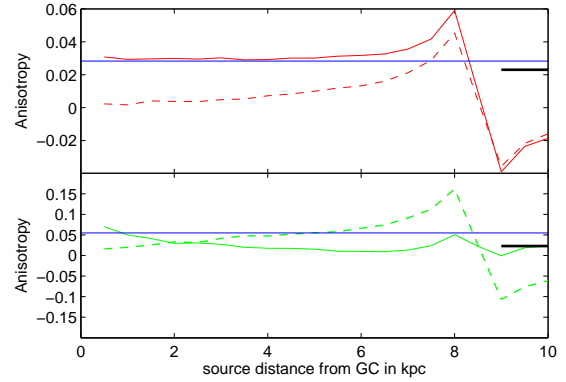


Figure 2: Anisotropy in flux from the ring-like sources is plotted as a function of distance of the rings from the GC in the test particle simulation. The solid curve is for the radial anisotropy and the dashed curve is for the anisotropy along the z direction. The solid blue lines indicate the total anisotropy expected at Earth after summing over contribution from all ring-like sources in the Galaxy. The top panel is for $\lambda_{mfp} = r_L(B_0)$ and in the bottom panel $\lambda_{mfp} = 3r_L(B_0)$

z_0	$\lambda_{mfp} = r_L(B_0)$			$\lambda_{mfp} = 3r_L(B_0)$		
	δ_r	δ_z	δ_{tot}	δ_r	δ_z	δ_{tot}
$B_{\phi}^z(z) = \exp(- z /z_0)$						
1.5	2.6%	1.0%	2.8%	2.1%	5.0%	5.5%
3	2.4%	1.4%	2.8%	-0.1%	2.8%	2.8%
$B_{\phi}^z(z) = 1/(1+ z /z_0)$						
1.5	2.4%	1.3%	2.7%	-1%	2.9%	3.0%
3	2.4%	1.5%	2.8%	0%	2.6%	2.6%
10	2.3%	1.5%	2.7%	1.1%	2.4%	2.7%

Table 1: Anisotropy for different configurations of the GMF in the test particle simulation. The mean free path is assumed to be Larmor radius $r_L(B_0)$ in magnetic field $B_0=10 \mu G$

1. Recent reports of Fermi bubble in different wavelengths suggest a strong magnetic field upto 15 microgauss [e.g. 8] close to the Galactic center. Since the contribution of sources close to the Galactic center to the UHECRs flux at Earth is negligible, our results would be unaffected by the details of GMF close to the Galactic center, and has not been considered in the present analysis.

z_0 in Kpc	$\lambda_{mfp} = r_L$			$\lambda_{mfp} = 3r_L$		
	δ_r	δ_z	δ_{tot}	δ_r	δ_z	δ_{tot}
$B_\phi^z(z) = \exp(- z /z_0)$						
1.5	1.4%	1.3%	1.9%	-1%	3.2%	3.3%
3	1.3%	1.1%	1.7%	0.2%	2.7%	2.7%
$B_\phi^z(z) = 1/(1+ z /z_0)$						
1.5	1.2%	1.1%	1.7%	-1%	2.9%	3.0%
3	1.2%	1.0%	1.6%	0.2%	2.5%	2.5%
10	1.1%	0.9%	1.5%	1.0%	2.1%	2.3%

Table 2: Anisotropy, as in the table 1, for different configurations of the GMF in the test particle simulation. Here the mean free path of UHECRs is local Larmor radius in the GMF.

If the mean free path is assumed to scale as local Larmor radius, then the anisotropy falls well within the observed limit (Table 2) for Bohmian diffusion ($\lambda_{mfp} = r_L$). This is because the spatial variation of the diffusion coefficient causes the CRs to escape more rapidly, so that we get significant contribution only from very nearby sources (On the other hand, this raises the discreteness anisotropy). If the mean free path is increased to $3r_L$, thus making the diffusion anisotropic, the UHECR anisotropy goes up because of increased drift. Altogether, these cases demonstrate that the drift has significant contribution to the total anisotropy, generally pushing it beyond the observed limits, unless it is suppressed by rapid scattering near the Bohm limit, or by a nearly uniform distribution of sources.

3 Discussion and Conclusions

We have calculated the time-dependent transport of UHECRs from a point-like instantaneous sources, assuming that the transport rates are different along and across the toroidal GMF (isotropic diffusion, discussed in PE11, being a special case when both are equal). We showed that the regular component of the GMF would make the transport of UHECRs in the Galaxy anisotropic with respect to their sources, which in turn would affect the observed anisotropy of UHECR flux at Earth.

The dependence of time averaged anisotropy on D_{\parallel} and D_{\perp} would depend upon the distribution of sources and their rate in the Galaxy and . Considering the sources distribution given by eq 4, we have shown the dependence of anisotropy on energy for isotropic (case 1) and anisotropic(case 3) diffusion, assuming $\lambda_{mfp}(\propto D_{\perp}) \propto E$, in figure 3 and 4.

As evident from figure 1, 3 and 4, mean and median of the anisotropy computed in the Monte carlo solution is significantly lower for anisotropic diffusion as compared to the isotropic diffusion. Assuming that a GRB occurs in every 1 Myr in the galaxy and their distribution follows eq. 4, the anisotropy falls below the observationally imposed 99% upper limit² for the energy band between 2 and 4 EeV of 2.3% during about 40% of the time for diffusion parameters as in case 3 (as compared to 25% of time if the diffusion is isotropic), strengthening our argument that the current value of UHECRs anisotropy is possible because of intermittency of UHECRs flux. However, if the distribution of sources follow eq. 4 or similar, a higher rate of sources in the Galaxy would mean increased level of anisotropy in

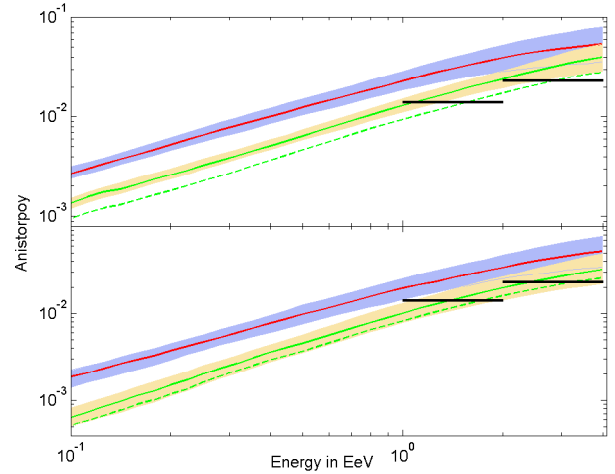


Figure 3: The median of anisotropy is plotted against the energy of UHECRs for source rate 1 per Myr. The upper (red) curve is for isotropic (case 1) and the lower (green) curve is for anisotropic diffusion (case 3). Top panel shows anisotropy for the source distribution given by eq. 4 and the bottom panel is for the uniform source distribution. The coloured regions indicate 68% containment region for the anisotropy at the given energy and the black bars indicate the measured 99% upper limit by the Auger collaboration. Dashed (green) curve indicates the median anisotropy for anisotropic diffusion if the contribution of drift is not included.

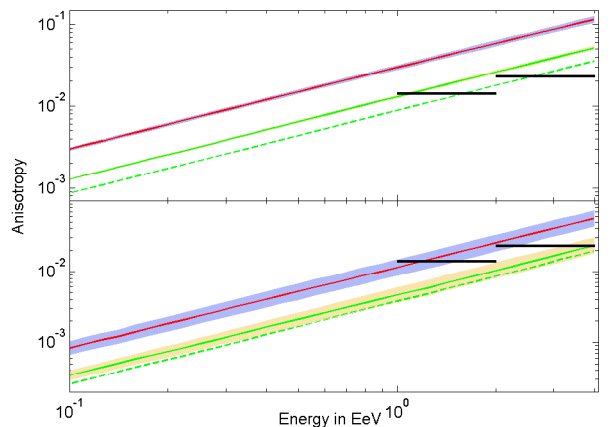


Figure 4: As in the figure 3, the median of anisotropy is plotted against the energy of UHECRs. Here the source rate is 1 per 10 kyr.

2. Recent analysis of Auger data suggests a slightly higher upper limit [18] 2.8%. However, we have adopted a previously reported stricter limit of 2.3%.

2 to 4 EeV energy band (top panel, fig. 4), as well as decrease in variance of the anisotropy.

On the other hand, a uniform or nearly uniform distribution of sources in the galaxy and/or heavier composition of UHECRs provides an alternative solution to the isotropy problem (bottom panels, fig. 3 and 4). As seen in table 3, there also exists the possibility that a very short (Bohmian) mean free path, in which the systemic anisotropy is reduced because only very nearby sources contribute. However, this raises the discreteness anisotropy, so it is not clear that any of the alternative solutions to intermittency are as attractive.

We acknowledge support from the Israel-U.S. Binational Science foundation, the Israeli Science Foundation, and the Joan and Robert Arnow Chair of Theoretical Astrophysics.

References

- [1] R. U. Abbasi, T. Abu-Zayyad, M. Al-Seady, M. Allen, J. F. Amman, R. J. Anderson, G. Archbold, K. Belov, J. W. Belz, D. R. Bergman, S. A. Blake, O. A. Brusova, G. W. Burt, C. Cannon, Z. Cao, W. Deng, Y. Fedorova, C. B. Finley, R. C. Gray, W. F. Hanlon, C. M. Hoffman, M. H. Holzschneider, G. Hughes, P. Hütemeyer, D. Ivanov, B. F. Jones, C. C. H. Jui, K. Kim, M. A. Kirn, E. C. Loh, J. Liu, J. P. Lundquist, M. M. Maestas, N. Manago, L. J. Marek, K. Martens, J. A. J. Matthews, J. N. Matthews, S. A. Moore, A. O'Neill, C. A. Painter, L. Perera, K. Reil, R. Riehle, M. Roberts, D. Rodriguez, N. Sasaki, S. R. Schnetzer, L. M. Scott, G. Sinnis, J. D. Smith, P. Sokolsky, C. Song, R. W. Springer, B. T. Stokes, S. Stratton, S. B. Thomas, J. R. Thomas, G. B. Thomson, D. Tupa, A. Zech, and X. Zhang. Indications of proton-dominated cosmic-ray composition above 1.6 eev. *Phys. Rev. Lett.*, 104:161101, Apr 2010.
- [2] A. A. Abdo, M. Ackermann, M. Ajello, W. B. Atwood, M. Axelsson, L. Baldini, J. Ballet, D. L. Band, G. Barbiellini, D. Bastieri, and et al. Fermi/Large Area Telescope Bright Gamma-Ray Source List. , 183:46–66, July 2009.
- [3] J. Abraham, P. Abreu, M. Aglietta, E. J. Ahn, D. Allard, I. Allekotte, J. Allen, J. Alvarez-Muñiz, M. Ambrosio, and Anchordoqui. Measurement of the depth of maximum of extensive air showers above 10^{18} eV. *Phys. Rev. Lett.*, 104:091101, Mar 2010.
- [4] W. I. Axford. The modulation of galactic cosmic rays in the interplanetary medium. , 13:115, February 1965.
- [5] V. S. Berezhinskii and S. I. Grigoreva. The Ultrahigh Energy Cosmic-Ray Spectrum. *Soviet Astronomy Letters*, 14:1, February 1988.
- [6] R. A. Burger, H. Moraal, and G. M. Webb. Drift theory of charged particles in electric and magnetic fields. , 116:107–129, November 1985.
- [7] Antoine Calvez, Alexander Kusenko, and Shigehiro Nagataki. Role of galactic sources and magnetic fields in forming the observed energy-dependent composition of ultrahigh-energy cosmic rays. *Phys. Rev. Lett.*, 105:091101, Aug 2010.
- [8] E. Carretti, R. M. Crocker, L. Staveley-Smith, M. Haverkorn, C. Purcell, B. M. Gaensler, G. Bernardi, M. J. Kesteven, and S. Poppi. Giant magnetized outflows from the centre of the Milky Way. , 493:66–69, January 2013.
- [9] C. J. Cesarsky and H. J. Volk. Cosmic Ray Penetration into Molecular Clouds. , 70:367, November 1978.
- [10] Carmelo Evoli, Daniele Gaggero, Dario Grasso, and Luca Maccione. Common solution to the cosmic ray anisotropy and gradient problems. *Phys. Rev. Lett.*, 108:211102, May 2012.
- [11] G. Giacinti, M. Kachelrie, D.V. Semikoz, and G. Sigl. Cosmic ray anisotropy as signature for the transition from galactic to extragalactic cosmic rays. *Journal of Cosmology and Astroparticle Physics*, 2012(07):031, 2012.
- [12] C.-Y. Huang, S.-E. Park, M. Pohl, and C. D. Daniels. Gamma-rays produced in cosmic-ray interactions and the TeV-band spectrum of RX J1713.7-3946. *Astroparticle Physics*, 27:429–439, June 2007.
- [13] J. R. Jokipii. Rate of energy gain and maximum energy in diffusive shock acceleration. , 313:842–846, February 1987.
- [14] P. O. Lagage and C. J. Cesarsky. The maximum energy of cosmic rays accelerated by supernova shocks. , 125:249–257, September 1983.
- [15] A. Levinson and D. Eichler. Baryon Purity in Cosmological Gamma-Ray Bursts as a Manifestation of Event Horizons. , 418:386, November 1993.
- [16] Pierre Auger Collaboration. Measurement of the energy spectrum of cosmic rays above 10^{18} eV using the Pierre Auger Observatory. *Physics Letters B*, 685:239–246, March 2010.
- [17] Pierre Auger Collaboration. Search for first harmonic modulation in the right ascension distribution of cosmic rays detected at the Pierre Auger Observatory. *Astroparticle Physics*, 34:627–639, March 2011.
- [18] Pierre Auger Collaboration, P. Abreu, M. Aglietta, M. Ahlers, E. J. Ahn, I. F. M. Albuquerque, D. Allard, I. Allekotte, J. Allen, P. Allison, and et al. Large-scale Distribution of Arrival Directions of Cosmic Rays Detected Above 10^{18} eV at the Pierre Auger Observatory. , 203:34, December 2012.
- [19] M. Pohl and D. Eichler. Origin of Ultra-high-energy Galactic Cosmic Rays: The Isotropy Problem. , 742:114, December 2011.
- [20] X. H. Sun, W. Reich, A. Waelkens, and T. A. Enßlin. Radio observational constraints on Galactic 3D-emission models. , 477:573–592, January 2008.
- [21] E. G. Zweibel and A. Brandenburg. Current Sheet Formation in the Interstellar Medium. , 478:563, March 1997.